Journal of Structural Geology 57 (2013) 58–80

Contents lists available at ScienceDirect

Journal of Structural Geology

journal homepage: www.elsevier.com/locate/jsg

Clay-smear continuity and normal fault zone geometry – First results from excavated sandbox models

S. Noorsalehi-Garakani [a,*], G.J. Kleine Vennekate [b], P. Vrolijk [c], J.L. Urai [a]

[a] Structural Geology, Tectonics and Geomechanics, RWTH Aachen University, Lochnerstraße 4-20, 52066 Aachen, Germany
[b] Chair of Geotechnical Engineering, RWTH Aachen University, Mies-van-der-Rohe-Str. 1, 52074 Aachen, Germany
[c] ExxonMobil Upstream Research Company, Houston, TX, USA

A R T I C L E I N F O

Article history:
Received 9 November 2012
Received in revised form
20 September 2013
Accepted 25 September 2013
Available online 8 October 2013

Keywords:
Sandbox
Clay-smear
Clay gouge
Shear-induced mixing
Deformation band architecture
Fault gouge evolution

A B S T R A C T

The continuity of clay-rich fault gouge has a large effect on fluid transmissibility of faults in sand–clay sequences, but clay gouge continuity and composition in 3D are not well known. We report observations of 3D clay smear continuity in water-saturated sandbox experiments where the sheared clay layers were excavated after deformation. The experiments build on existing work on the evolution of clay gouge in similar 2D experiments where interpretations were made in profile view.

We used well-known model materials ("Benchmark" sand and uncemented kaolinite–sand mixtures) that were further characterized using standardized geotechnical tests and triaxial compression experiments at effective pressures corresponding to the sandbox experiments. Results show a nonlinear failure envelope of the sand, in agreement with existing models. Unconfined compression experiments with the clay show cohesion around 50 Pa and brittle behavior.

A sheared, ductile clay layer embedded in sand above a 70° dipping basement fault reveals a complex, natural-looking clay gouge architecture with relay ramps, breached relays and fault lenses. The clay gouge shows clear variations in composition and thickness and becomes locally discontinuous at throw-thickness ratios above 7, in contrast to our earlier 2D observations where discontinuous clay-gouge only formed in cemented clay layers. In addition to tectonic telescoping in the relays, the thin, continuous parts of the clay gouge were transformed from an initial pure clay by mechanical mixing of sand and clay.

We also discuss the applicability of these results to the evolution of normal fault zones and deformation bands in sand–clay sequences at effective pressures below the onset of cataclasis and conclude that in fault zones a higher degree of internal segmentation reduces the probability of the formation of discontinuities.

1. Introduction

The transport properties of clay-rich normal fault zones in sand–clay sequences are of considerable practical importance and have been investigated in outcrop, in the subsurface and in numerical and analog models, but the multitude of nonlinear processes and feedback systems together with poorly constrained sedimentary architecture and rock properties make quantitative prediction difficult (e.g. Lehner and Pilaar, 1991; Yielding et al., 1997; Clausen and Gabrielsen, 2002; Van der Zee et al., 2003, 2005; Egholm et al., 2008; Urai et al., 2008; Wibberley et al., 2008; Schmatz et al., 2010a,b; Nollet et al., 2012; Yielding, 2012). Since the permeability of continuous clay gouge is very low in comparison with that of sand (e.g. Holland et al., 2006; Crawford et al., 2008; Cuisiat and Skurtveit, 2010), the amount of continuous clay incorporated into fault zones in sand–clay or sand–shale sequences is one of the main controlling factors for the fluid transmissibility of such faults.

In applied studies, empirical models were developed to predict the amount of clay in faults in the subsurface, for example shale gouge ratio (SGR), effective shale gouge ratio (ESGR), clay smear potential (CSP), and shale smear factor (SSF) (Yielding et al., 1997, 2010; Yielding, 2002). The central assumption of these models is that the fault gouge consists of a reworked equivalent of the wall rocks in the deformed interval. Local variations in the hydrologic integrity and composition of the fault gouge are often calibrated

* Corresponding author. Tel.: +49 241 80 98443.
E-mail addresses: s.noorsalehi@ged.rwth-aachen.de (S. Noorsalehi-Garakani), vennekate@geotechnik.rwth-aachen.de (G.J. Kleine Vennekate), peter.vrolijk@exxonmobil.com (P. Vrolijk), j.urai@ged.rwth-aachen.de (J.L. Urai).

0191-8141/$ – see front matter
http://dx.doi.org/10.1016/j.jsg.2013.09.008

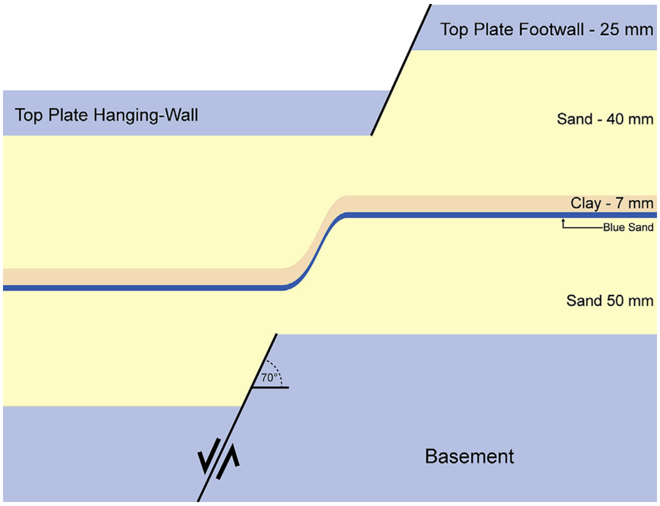

Fig. 1. Sketch of sandbox experiments (see also Schmatz et al., 2010a) and the geometry of all models presented in this paper.

using subsurface pressure and structural data. A deeper understanding of the clay smear processes and the internal structure of clay-rich gouge would provide a basis for an improvement of these predictions (Holland et al., 2006; Van der Zee and Urai, 2005).

In heterogeneously layered sequences with a competence contrast, faults develop from coalescing and propagating segments (Peacock and Sanderson, 1992; Childs et al., 1996), and fault segments were proposed to strongly influence clay gouge structure (Van der Zee et al., 2003). Other studies propose a “clay injection” process that leads to enrichment of the fault with clay to a greater extent than expected by shearing and reworking (Lehner and Pilaar, 1997). Another process of clay enrichment in normal faults is the vertical transport of clay along dilatant faults in brittle carbonates (Van Gent et al., 2010a,b).

The strong dependency of clay smear evolution on the mechanical properties of the material was shown in Sperrevik et al. (2000), Clausen and Gabrielsen (2002), Cuisiat and Skurtveit (2010) and Schmatz et al. (2010a,b). In general, a more continuous clay smear is formed with increasing effective stress and decreasing strength of the clay, mainly because both processes

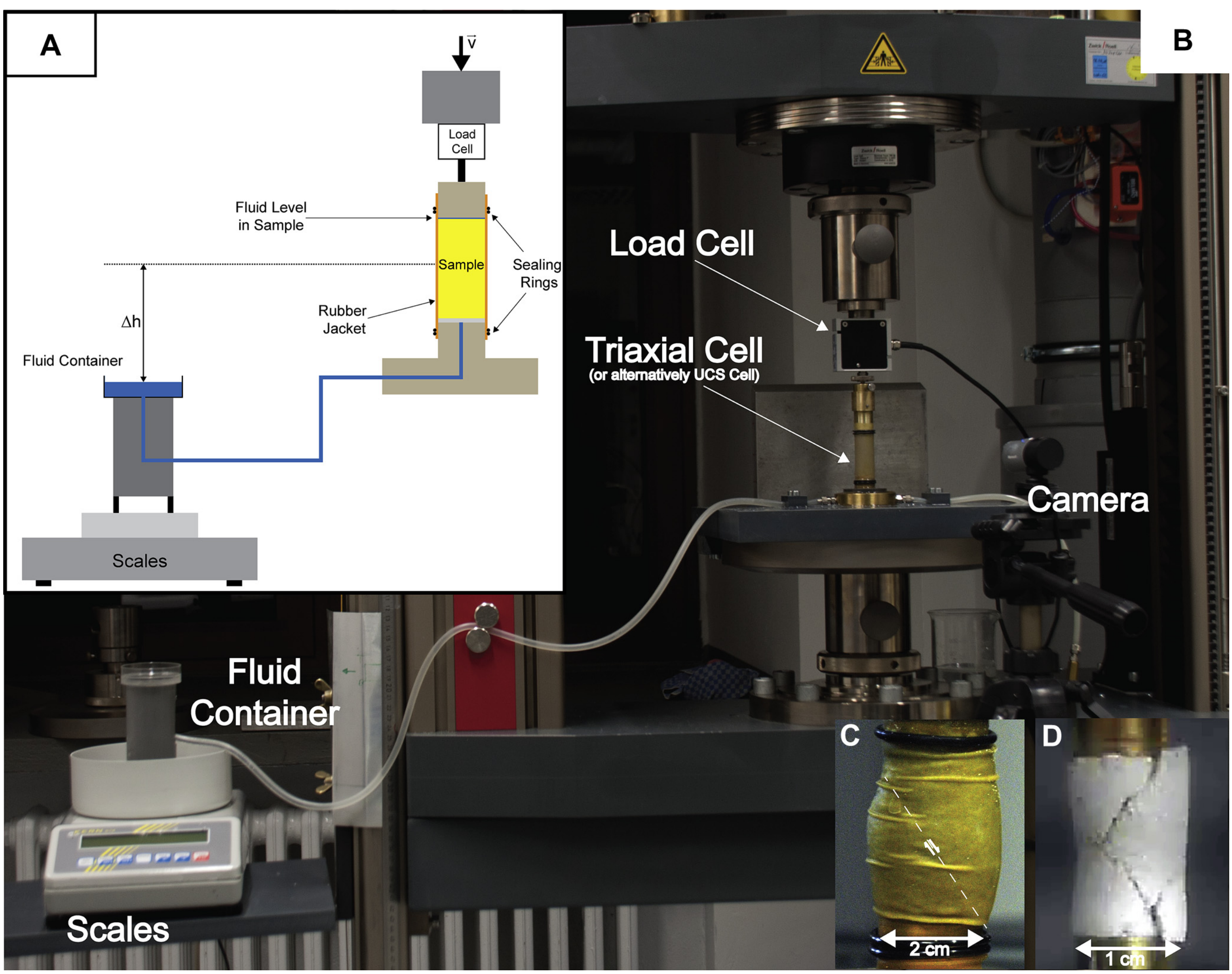

Fig. 2. A. Overview of the setup of the small-stress testing apparatus (B). C. Example of a jacketed sand sample at the end of deformation. D. Uniaxially compressed clay sample deformed unjacketed under water, showing brittle deformation.